Research Article

Journal of Molecular Recognition

Received: 9 April 2008, Revised: 10 April 2008, Accepted: 11 April 2008, Published online in Wiley InterScience: 5 August 2008

(www.interscience.wiley.com) DOI:10.1002/jmr.907

Piezoelectric biosensors assisted with electroacoustic impedance spectroscopy: a tool for accurate quantitative molecular recognition analysis

João M. Encarnação[a], Raul Baltazar[a], Peter Stallinga[b] and Guilherme N. M. Ferreira[a]*

In this work, electroacoustic impedance analysis based on a modified Butterworth–Van Dyke (BVD) model is used to complement resonance frequency measurements of piezoelectric crystal sensors for the identification and removal of interfering signals. This approach enables the accurate use of the Sauerbrey correlation to establish a direct relationship between mass deposited at the sensor surface and measured frequency variations. Kinetic models can thus be evaluated and binding constants estimated directly from the measured data. We further demonstrate the usefulness of this approach by applying it to the study of the formation of 11-hydroxy-1-undecanothiol self-assembled monolayers (SAM) as well as to the binding of streptavidin to immobilized biotin. Kinetic and equilibrium parameters were estimated from transient analysis, adsorption isotherms, Scatchard and Hill plots obtained from the frequency data for both the alkanethiol and streptavidin films.

This strategy based on electroacoustic impedance assisted quartz-crystal microbalance (QCM) biosensors is expected to be a major contribution for the use of these piezoelectric devices as a reliable and cheap detection system that can easily be integrated into analytical techniques. Copyright © 2008 John Wiley & Sons, Ltd.

Keywords: piezoelectric biosensor; impedance analysis; equivalent circuit; interferences; molecular interactions; affinity constants

INTRODUCTION

Piezoelectric sensors are an example of a simple and low cost detection system that can compete with the most common instrumentation used, particularly with application to biomolecules. Piezoelectric transduction enables label-free detection of biorecognition events and has been used in microgravimetric devices, generally known as quartz-crystal microbalance (QCM), for different applications (Yang *et al*., 1998; Etchenique and Brudny, 2000; Liu *et al*., 2004; Su and Li, 2005; Wu *et al*., 2005; Modin *et al*., 2006; Encarnação *et al*., 2007a; Ferreira *et al*., 2007; Mitomo *et al*., 2007). These sensors are driven to mechanically resonate at a particular frequency (f_0) (Köβlinger *et al*., 1995; Laricchia-Robbio and Revoltella, 2004), that is dependent on the deposition of mass according to the Sauerbrey equation (Sauerbrey, 1959) (Equation (1)).

$$\Delta f_m = -\frac{2nf_0^2}{\sqrt{\rho_q \mu_q}} \frac{\Delta m}{A} \quad (1)$$

where Δf_m is the frequency change due to mass loading, f_0 the resonant frequency of the fundamental mode, n the overtone ($n = 1$ for the fundamental mode), ρ_q and μ_q are the density and the shear mode of the quartz material, respectively, Δm is the mass change and A the sensor sensitive area. Equation (1) is only valid for thin, rigid and uniform films. If the surface film is not entirely rigid, or when measurements are carried out in liquid environments, the quartz response depends not only on the mass load but also on the properties of the attached layer and buffers (Etchenique and Weisz, 1999; Etchenique and Buhse, 2000; Lucklum and Hauptmann, 2000; Ghafouri and Thompson, 2001; Encarnação *et al*., 2007b). Analyte detection in liquid environments is thus influenced by these interferences, resulting in non-mass-related resonance frequency variations which are additive to Δf_m (Encarnação *et al*., 2007b). Mass variations cannot be differentiated when only the frequency change is measured, and, therefore, one has to be extremely careful when evaluating and interpreting the resonance frequency data. Despite the recent increase of publications regarding the use of quartz crystal sensors for molecular recognition (Cooper and Singleton, 2007), the true analytical potential of these devices is still compromised by these interferences.

In this work, we demonstrate the potential of piezoelectric sensors assisted with electroacoustic impedance analysis for

* *Correspondence to: G. N. M. Ferreira, IBB-Institute for Biotechnology and Bioengineering, Centre for Molecular and Structural Biomedicine, University of Algarve, 8000-117 Faro, Portugal.*
E-mail: gferrei@ualg.pt

a *J. M. Encarnação, R. Baltazar, G. N. M. Ferreira*
IBB-Institute for Biotechnology and Bioengineering, Centre for Molecular and Structural Biomedicine, University of Algarve, 8000-117 Faro, Portugal

b *P. Stallinga*
Centre for Electronics, Optoelectronics and Telecommunications, University of Algarve, 8000-117 Faro, Portugal

quantitative molecular detection and measurements in liquid environments. Real-time impedance analysis is performed to identify interferences and to assess their influence to the sensor signal, particularly viscoelastic and charge effects (Martin *et al.*, 1991; Auge *et al.*, 1995; Bouché-Pillon *et al.*, 1995; Etchenique and Weisz, 1999; Lucklum and Hauptmann, 2000; Zhou *et al.*, 2000; Encarnação *et al.*, 2007b). The methodology used is based on a modified Butterworth–Van Dyke (BVD) equivalent electrical circuit model (Encarnação *et al.*, 2007b) (Figure 1), where each circuit parameter is related to a physical aspect of the sensor resonance. These parameters can be estimated from the acoustic impedance measured near the sensor fundamental resonance frequency ($f = (4\pi^2 L_m C_m)^{-1/2}$). The use of correlations to account for the influence to the sensor resonance frequency by the resistive component, owing to viscoelastic effects (Martin *et al.*, 1991; Zhou *et al.*, 2000) and by the parallel capacitive component (Encarnação *et al.*, 2007b), due to the influence of charges, enables the elimination of these interferences and the exact quantification of the deposited mass by the Sauerbrey equation (Encarnação *et al.*, 2007a, Ferreira *et al.*, 2007).

This strategy can contribute to validate a quantitative analytical methodology based on a specific piezoelectric biosensor. The applicability of this approach is demonstrated by following the known mechanisms of the formation of alkanethiol self-assembled monolayers (SAM) and the binding of streptavidin to biotin-modified sensors. We demonstrate that resonance frequency signal can be deconvoluted using electroacoustic impedance data to identify and assess the influence of interferences. The calculation of kinetic data directly from the measured data is thereby enabled while simultaneously pointing to the possible molecular mechanisms involved.

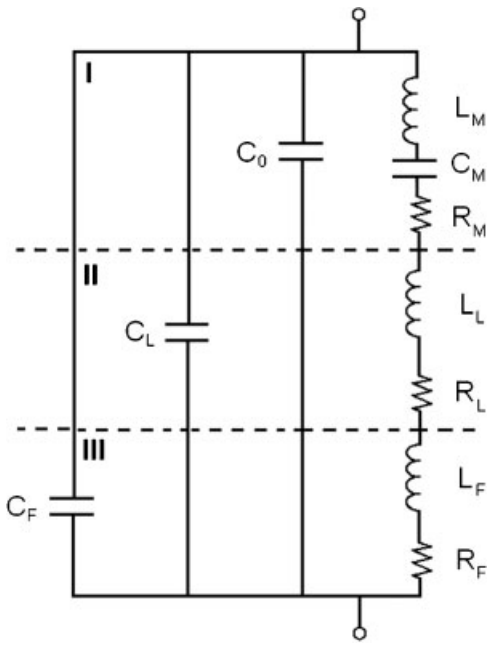

Figure 1. Butterworth–van Dyke equivalent circuit model of QCM sensors (I) unloaded resonator (II) elements added due to liquid medium exposure; and (III) elements added due to the adsorption of mass on the surface of the sensor. The static capacitance C_0 accounts for parasitic capacitance due to electrodes, charge variations, holding structure and cables; the inductive component (L_m) is related to inertial forces to oscillation, and thus related to mass dislocation; the motional capacitance (C_m) accounts for the oscillation energy storage related to the crystal's elasticity; the resistance (R_m) is related to the energy dissipation owing to viscoelastic phenomena in viscous solutions and viscoelastic films; C_L and C_F represent the stray capacitance generated, respectively, by the liquid medium and the deposited film.

MATERIALS AND METHODS

Reagents

All chemicals and reagents were ultra-pure, pro-analysis or equivalent grade. Milli-Q water was used.

Sodium dihydrogen phosphate, disodium hydrogen phosphate, sodium chloride, ethanolamine, sulphuric acid and hydrogen peroxide were purchased from Merck. Absolute ethanol and dimethyl formamide (DMF) were purchased from Riedel-de-Häen.

Dithiobis succinimidyl undecanoate (DSU) and 11-hydroxy-1-undecanothiol were purchased from Dojindo Molecular Technologies.

Streptavidin was purchased from Roche and biotinyl-3,6-dioxaoctanediamine was purchased from Pierce.

Quartz crystal sensors

AT-cut quartz crystals (5 MHz; 2.54 cm diameter), coated with optically flat polished gold electrodes on both sides, were purchased from Stanford Research Systems (SRS, Stanford, USA). The active area and sensitivity factor of the crystal are $A = 0.4\ cm^2$ and $C_f = 56.6\ Hz\ cm^2\ \mu g^{-1}$, respectively.

The crystals were cleaned before use by rinsing with absolute ethanol and Milli-Q water followed by immersion in Piranha solution (3:1 mixture of sulphuric acid and 30%, hydrogen peroxide) for 15 min, to obtain a clean gold surface. Cleaned crystals were then rinsed with water and dried in a nitrogen stream.

Quartz crystal sensor functionalization with biotin

First, 30 μl of a 100 μM solution of DSU, prepared in DMF, were pipetted onto the surface of a cleaned crystal sensor, and incubated at room temperature for 2 h. Unbound DSU was removed by washing the functionalized crystal sensors sequentially with DMF and Milli-Q water.

After drying under a nitrogen flow, the functionalized crystal sensors were incubated for 2 h, at room temperature in a humidified chamber, with 50 μl of a 50 μM 11-hydroxy-1-undecanothiol ethanolic solution. After washing with absolute ethanol, Milli-Q water and drying under a nitrogen flow, the functionalized crystal sensors were incubated for 2 h at room temperature, with 30 μl of a 200 $\mu g\ ml^{-1}$ solution of biotin prepared in PBS buffer (100 mM NaCl, pH 7.4). Unbound or physisorbed molecules were removed by washing the functionalized crystal sensors sequentially with PBS buffer and Milli-Q water. To avoid the possibility of target molecules to directly react with the mixed SAM, the free DSU molecules were blocked by depositing 50 μl of ethanolamine solution, on top of the metal electrodes for a period of 2 h.

Experimental set-up

Cleaned or functionalized sensors were mounted on a Kynar crystal holder (SRS) with a home made acrylic cover to form a 300 μl flow cell exposing just one face of the sensor to the solution.

Viton O-rings were placed underneath the sensor, sealing the flow cell to avoid wetting or flooding the electrical contacts located on the bottom of the crystal holder. A closed-cycle fluidic circuit was mounted using Tygon tubing to connect the flow cell to an agitated container where all the samples are added. The total volume of the system is 2 ml and the solutions were re-circulated in the system at a flow rate of 1.5 ml min^{-1} controlled by a Watson-Marlow peristaltic pump. Both the flow cell and the container were installed in a home made 1 L-jacketed beaker to control the temperature of the system at $25 \pm 0.1^{\circ}C$ by means of a Thermo Haake temperature controller.

The resonance frequency and impedance spectra were recorded alternatingly using a QCM100 Controller and a QCM25 Oscillator (SRS) connected to a Pendulum CNT-66 frequency counter or using a RF HP8712C Network Analyzer, respectively. The network analyzer and the QCM25 Oscillator were electrically connected to the crystal holder through an electronic switch used to select the desired measurement mode. The instruments were interfaced to a computer through IEEE boards and custom made acquisition programmes.

Impedance analysis

Impedance spectra were obtained using a 10 kHz frequency span centred near the crystal's resonant frequency with 16 spectra averaging at 1 Hz resolution.

The BVD equivalent circuit parameters were obtained from the experimental data by calculating the conductance function ($|Y|=|Z|^{-1}$; $|Z|$ being the recorded impedance magnitude) and fitting, using a fitting routine written in Matlab, to the following equations:

$$|Y| = \sqrt{\left(\frac{R_m}{R_m^2 + U^2}\right)^2 + \left(\omega C_0 - \frac{U}{R_m^2 + U^2}\right)^2} \quad (2)$$

$$U = \omega L_m - \frac{1}{\omega C_m} \quad (3)$$

where $\omega = 2\pi f$ is the angular frequency.

The analysis is initialized by estimating the four BVD parameters (R_m, L_m, C_m and C_0) for the crystal sensor exposed to air. Typical parameters for air exposed crystal sensors in the experimental set-up used are $R_m = 12.925\,\Omega$, $L_m = 33.725$ mH, $C_m = 29.925$ fF and $C_0 = 184.575$ pF, respectively. Since C_m is related only to the sensor physical material, it is constant within the experiments. The successive contributions of solvents and adsorbed mass are thus obtained by a three parameter fitting (R_m, L_m, C_0) of the respective conductance functions (Encarnação *et al*., 2007b). This procedure is repeated for each stage of the experiment and the BVD parameters of the particular experimental stage, thus of the individual contributions, are calculated by subtracting the global parameters, obtained by fitting, from the respective parameter calculated for the previous stage of the experiment (Encarnação *et al*., 2007a, 2007b; Ferreira *et al*., 2007). To facilitate data analysis it is usual to represent a parameter *XL* which is the sensor inductance in resistive units (Ω) obtained by multiplying the calculated inductance value by the angular frequency $\omega = 2\pi f$.

Calculation of binding kinetic constants

The kinetic constants were calculated from frequency transients by nonlinear fitting to a 1:1 binding model as shown in the following equation:

$$\frac{d\theta}{dt} = k_1(1-\theta)C - k_{-1}\theta \quad (4)$$

where θ is the surface coverage, C the initial ligand concentration and k_1 and k_{-1} are the association and dissociation rate constants, respectively. Upon integration of the rate equation (Equation (4)), an expression is obtained to describe the time dependency of the sensor surface coverage

$$\theta = \frac{C}{C + \frac{k_{-1}}{k_1}}\theta_\infty[1 - \exp[-t/\tau]] \quad (5)$$

where θ_∞ is the total available binding sites at the sensor surface and $\tau = [k_1 C + k_{-1}]^{-1}$ is the relaxation time of binding. The rate constants k_1 and k_{-1} are then calculated from the slope and intercept of linear regression of the reciprocal of the relaxation time variation with the ligand concentration.

RESULTS AND DISCUSSION

Formation of self-assembled monolayer (SAM)

Alkanethiols are known to spontaneously adsorb to gold surfaces self-assembling as oriented monolayers. Alkanethiol self-assembly is initiated by the strong chemical interaction between the sulphur and the metal surface (Karpovich and Blanchard, 1994) which is followed by lateral interactions of neighbour adsorbed molecules, leading to the parallel alignment of the molecules generating a thin, rigid and uniform film at the sensor surface (Liao *et al*., 2000). We thus selected the formation of alkanethiol SAMs to illustrate the use of piezoelectric sensors in quantitative monitoring of thin, rigid, films within the assumptions of the Sauerbrey equation.

Increasing concentrations of 11-hydroxy-1-undecanothiol were re-circulated over the sensor surface and the frequency variation was measured (Figure 2A). Time-dependent resonance frequency transients indicate alkanethiols adsorption, which occurs rapidly up to the establishment of an equilibrium (Figure 2A). Three distinct regions are identified in the adsorption transients (Figure 2A): an initial period (region I), characterized by excess surface binding sites to which alkanethiols adsorb very rapidly; in region II (Figure 2A), fewer binding sites are available as the surface is closer to the saturation. This region is characterized by a slow organization of the SAM which may result in the release of excess adsorbed molecules as shown for the higher alkanethiol concentrations; Finally, region III corresponds to the equilibrium of the chemisorption process. As shown in Figure 2A, steeper frequency transients are obtained for higher alkanethiol concentrations and alkanethiol adsorption follows a standard saturation-like isotherm (Figure 2B). When analysing these data using a Langmuir isotherm, sensor saturation at $\sim 58 \pm 5$ Hz and a dissociation constant of $\sim 69 \pm 16\,\mu$M were calculated. Even though acceptable distribution of the residuals is obtained (Figure 2C) and data fitting to Langmuir isotherm is accepted by the χ^2 statistical test (95% confidence level and 5 degrees of freedom), significant deviations are shown (Figure 2B) which reveals the possible influence of molecular phenomena, such as mass transfer and cooperativity, which are not predicted in the Langmuir model. While no conclusion may be taken regarding the influence of mass transfer, the convex shape of the Scatchard plot (Figure 2D) indicates positive cooperative effects during the

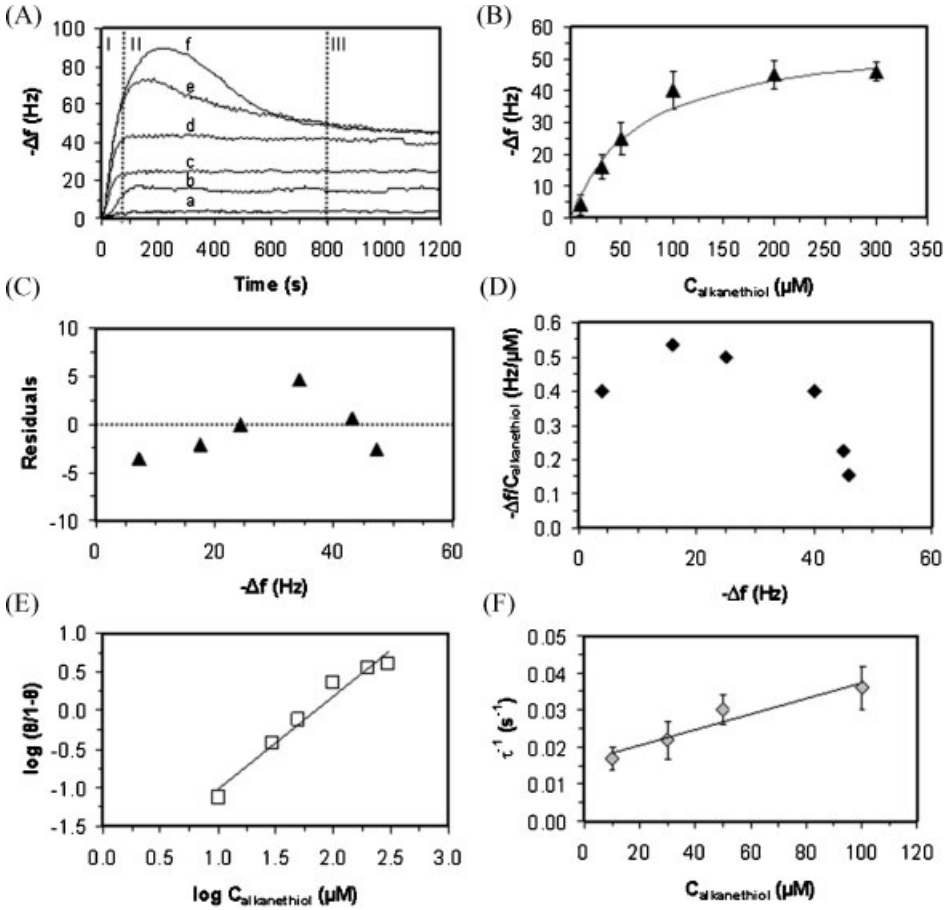

Figure 2. (A) Frequency shift response of quartz crystal gold sensors to the exposure to increasing bulk concentrations (a—10 μM; b—30 μM; c—50 μM; d—100 μM; e—200 μM; f—300 μM) of 11-hydroxy-1-undecanothiol. (B) Saturation curve showing the total frequency shift obtained for each concentration of alkanethiol used. The curve represents the nonlinear interpolation of the data to the saturation component of the molecular model presented in Equation (5), with accepted goodness for $\chi^2 = 9.14 <$ critical $\chi^2 = 11.07$ ($\alpha = 0.05$, $n = 5$). (C) The residuals data for the interpolation presented in (B). (D) Scatchard plot and (E) Hill plot for the data presented in (B). (F) Linear dependence of the 1:1 molecular model calculated constant τ (relaxation time of binding), to the lowest bulk alkanethiol concentrations used (10–100 μM). Linear regression of experimental data yielded the correlation: $\tau = (2.1 \pm 0.4) \times 10^{-4}\,\mu M^{-1}\,s^{-1} \times C + (1.6 \pm 0.2) \times 10^{-2}\,s^{-1}$; $r = 0.9659$; ANOVA analysis accepts linear interpolation for F statistic $p = 0.034 < \alpha = 0.05$. Each presented data are the average result of three independent experiments.

adsorption process which is consistent with the three-stage mechanism proposed above. Positive cooperativity of alkanethiol adsorption is further demonstrated by the Hill coefficient ($n_H = 1.2 \pm 0.1$) obtained from the slope of the respective Hill plot—Figure 2E.

In order to evaluate the usefulness of frequency variation data to calculate the amount of mass adsorbed at the sensor surface by the Sauerbrey equation, the sensor acoustic impedance was measured at the end of each of the adsorption processes shown at Figure 2A. The acoustic impedance parameters were then estimated from impedance spectra using a BVD equivalent model (Table 1). As expected, increasing variations of the inductive component of the BVD model (ΔXL_F) were calculated as increasing mass amounts are adsorbed onto the sensor surface. On the other hand, the variation of both impedance resistance (ΔR_F) and capacitance (ΔC_F) were negligible indicating the formation of a rigid film with no charge influence. Therefore, no viscoelastic or charge interferences affect the measured frequency variation, and thus the Saurbrey equation can be directly applied to the measured frequency variation enabling adsorbed mass quantification (Table 1).

Alkanethiols are know to self-assemble onto gold surfaces forming a hexagonal-like structure (Porter *et al*., 1986; Strong and Whitesides, 1987). The distance between each adsorbed molecule is ~5 Å resulting in an available area for each molecule of ~21.4 Å^2 (Porter *et al*., 1986; Strong and Whitesides, 1987). Alkanethiol packaging in SAMs is also known to be size dependent. Alkathiols with higher chain lengths (typically > 9 CH_2 groups) tilt onto a certain degree regarding the surface, leading to higher surface densities with closer distances between each molecule (Porter *et al*., 1986; Strong and Whitesides, 1987). In the lower density limit mentioned above, one can estimate that a monolayer contains ~10^{14} immobilized molecules in the crystals active area. As shown in Table 1, the experimental values obtained for alkanthiol immobilization seems to converge to a value of similar order of magnitude. This is an additional indication of the effectiveness of this methodology to quantify mass, as monolayers of alkanethiols were quantitatively measured.

The validity of the Sauerbrey model demonstrated by the acoustic impedance analysis can also be used to estimate binding constants from transient data. According with the Sauerbrey

Table 1. Impedance analysis parameters calculated for 11-hydroxy-1-undecanothiol SAMs obtained with increasing bulk concentrations of alkanethiol, and respective immobilized mass calculated using the Sauerbrey model

Concentration (μM)	ΔXL_F (Ω)	ΔR_F (Ω)	ΔC_F (pF)	Immobilized mass (μg cm^{-2})	Number of immobilized molecules ($\times 10^{-14}$)*
10	1.8 ± 0.4	0.4 ± 0.2	0.08 ± 0.02	0.07 ± 0.05	0.9 ± 0.6
30	7.1 ± 0.8	1.0 ± 0.3	0.06 ± 0.01	0.28 ± 0.07	3.4 ± 0.9
50	11 ± 1	0.8 ± 0.4	0.06 ± 0.03	0.44 ± 0.09	5.3 ± 1
100	17 ± 1	1.5 ± 0.7	0.10 ± 0.06	0.7 ± 0.1	8.5 ± 1
200	19 ± 2	1.9 ± 0.6	0.11 ± 0.04	0.80 ± 0.08	9.8 ± 1
300	20 ± 2	1.8 ± 0.4	0.15 ± 0.09	0.81 ± 0.05	9.9 ± 0.6

*The sensor active area is 0.4 cm^2 as indicated in Materials and Methods.

equation, the sensor surface coverage (θ) is proportional to the measured frequency variation. Therefore, Equation (5) can be used to calculate the binding relaxation time (τ) from which the binding rate constants can be further calculated. However, as discussed above this model may not be appropriate to interpret the presented SAM formation. Nevertheless, given its simplicity this model was used within the linear region of the adsorption isotherm (up to 100 μM). As shown in Figure 2F, a plot of τ^{-1} versus C yields a straight line with slope $k_1 = 211 \pm 40\,M^{-1}\,s^{-1}$ and intercept $k_{-1} = (1.6 \pm 0.2) \times 10^{-2}\,s^{-1}$ from which a dissociation equilibrium constant $K_D = k_1/k_{-1} = (8 \pm 2) \times 10^{-5}$ M. Even though this dissociation equilibrium constant is ~20% higher from the one calculated from the isotherm, which may be the result of deviation from the ideality, as discussed previously, the rate constants calculated are consistent with previously published data for SAM of other alkanethiol molecules (Karpovich and Blanchard, 1994; Liao *et al*., 2000; Kim *et al*., 2001).

Piezoelectric detection and analysis of streptavidin binding to biotin

Streptavidin is a homotetrameric molecule folded in such a way that the four biotin binding sites are grouped in pairs located at opposite faces of the protein. The very high-specific binding affinity between streptavidin and its ligand biotin makes this system a very attractive model to study surface recognition processes (Muzykantov *et al*., 1994; Yao *et al*., 1995; Rosebrough and Hashmi, 1996; Schechter *et al*., 1999; Ewalt *et al*., 2001). Binding of streptavidin to immobilized biotin is known to result in well-ordered biofilms (Chilkoti *et al*., 1995; Qureshi *et al*., 2001), therefore, in this work streptavidin detection was selected to demonstrate the usefulness of piezoelectric sensors to specifically detect proteinaceous analytes in solution.

Piezoelectric sensors were functionalized with biotinyl-3,6-dioxaoctanediamine, mounted in the experimental set-up and used to detect streptavidin injected in the buffer flow.

As shown in Figure 3, the biofilm of immobilized biotin specifically captures streptavidin from solution, as no sensor response are obtained for a mixture of BSA, ribonuclease A and cytochrome *c* (Figure 3A), while significant frequency variations are monitored for streptavidin binding (Figure 3B). Figure 3A also includes controls to evaluate the eventual unspecific binding of streptavidin to any of the sensor surface component. As shown, no streptavidin binding is seen to clean or SAM-modified gold surfaces.

Streptavidin binding to biotin biofilms tends rapidly to the equilibrium according to a saturation isotherm (Figure 3C), with an acceptable distribution of the residuals (Figure 3D). As before, the data were fitted to a Langmuir isotherm yielding a saturation, capacity, corresponding to $\Delta f_{max} = (20.2 \pm 0.4)$ Hz and a dissociation equilibrium constant $K_D = ((5.8 \pm 0.7) \times 10^{-10}$ M) which is comparable to most of the published equilibrium constants (Table 2). Similarly, to the study of SAM formation, Scatchard plots and Hill analysis were performed to evaluate cooperative effects during streptavidin recognition (Figures 3E and F, respectively). The data indicate that streptavidin binding to immobilized biotin films is characterized by a negative cooperativity ($n_H = 0.69 \pm 0.07$). This result is consistent with binding mechanisms of biomolecule binding to natural receptors (Nesbitt *et al*., 1982; Chazenbalk *et al*., 1996; Urizar *et al*., 2005) where, upon binding, the formation of the affinity pair may partially or completely hinder adjacent binding sites (receptors).

Acoustic impedance analysis was performed to identify the presence of viscoelastic and charges interferences in the frequency variation transients obtained for streptavidin binding (Figure 4). As expected, the inductance variation (XL_F) follows a concentration-dependent trend similar to the adsorption isotherm obtained from frequency measurements, which reveals the binding of streptavidin to the immobilized biotin biofilms (Figure 4). Resonant energy dissipation due to viscoelastic interference can be neglected as indicated by the ~0 variation of the impedance resistance (ΔR_F). Viscoelastic effects, however, are observed for the highest streptavidin concentrations, which, according to the Martin model (Martin *et al*., 1991), $\Delta R = -4\pi L_m \Delta f_m$, results in a frequency variation interference of 2 Hz. Even though having some importance at the molecular level, the resulting viscoelastic interference results in a neglected frequency overestimation (positive value) since it is within the noise level, and thus the uncertainty, associated with the frequency measurements. Information concerning charge interferences is given by the parallel capacitance C_F, which results in desorption-like signals of 8.0 ± 0.5 Hz/pF (Encarnação *et al*., 2007b). As shown in Figure 4, the maximum capacitance variation monitored during streptavidin binding was (0.36 ± 0.06 pF) resulting in an equivalent to 3 Hz frequency underestimation (negative value) during frequency counting. Since viscoelastic and charge frequency interferences are additive (Encarnação *et al*., 2007b), the combined viscoelastic and charge effects result in a maximum 1 Hz interference which is within the instrumental resolution of frequency counting and noise level.

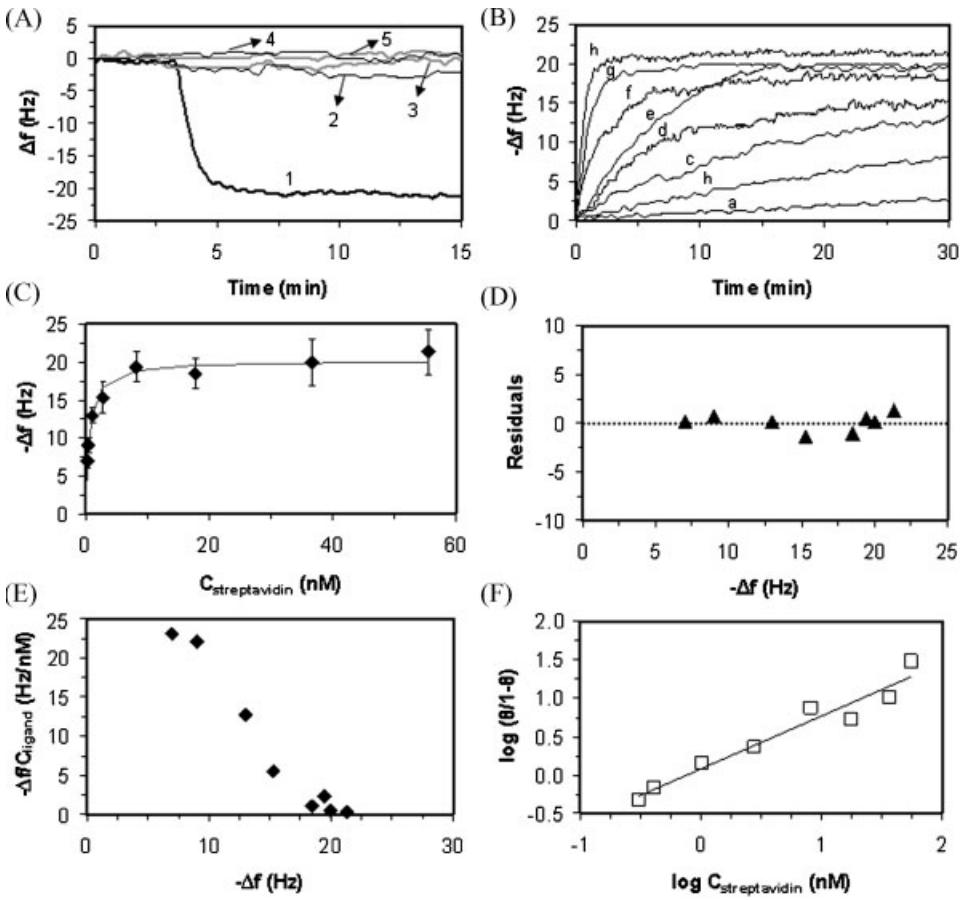

Figure 3. (A) Blank assays compared to biotin–streptavidin molecular recognition: (1) crystal with biotin exposed to streptavidin at 3 μg ml^{-1}, (2) crystal with biotin exposed to a mixture of BSA, ribonuclease A and cytochrome *c*, each protein at 50 μg ml^{-1} (3) clean crystal exposed to streptavidin at 3 μg ml^{-1}, (4) crystal with biotin exposed to PBS and (5) crystal with SAM exposed to streptavidin at 3 μg ml^{-1}. (B) Biotin functionalized QCM resonance frequency response, to different streptavidin concentrations (μg ml^{-1}): (a) 0.025, (b) 0.05, (c) 0.1, (d) 0.2, (e) 0. 5, (f) 1.0, (g) 2.0 and (h) 3.0. Each presented curve represents the average of three transients obtained experimentally. (C) Saturation curve showing the total frequency shift obtained for each concentration of streptavidin used. The curve represents the nonlinear fit of the data to the saturation component of the molecular model presented in Equation (5)—$\chi^2 = 0.79 <$ critical $\chi^2 = 14.07$ ($\alpha = 0.05$, $n = 7$). (D) Residuals of the data fitting presented in (C). (E) Scatchard plot and (F) Hill plot for the data presented in (C).

Hence, we can conclude from this acoustic impedance analysis that the Sauerbrey model can be used to relate frequency counting and mass quantification and therefore to quantitatively measure the amount of streptavidin as well as the streptavidin–biotin binding kinetics. Similarly to what was described for the SAM formation, upon fitting the frequency variation transients to a 1:1 binding model (Equation (5)), the association ($k_1 = (4.6 \pm 0.3) \times 10^5\,M^{-1}\,s^{-1}$) and dissociation

Table 2. Rate and equilibrium kinetic constants determined for the pair streptavidin–biotin in different published studies and in this work

$k_1 \times 10^{-7}$ ($M^{-1}\,s^{-1}$)	$k_{-1} \times 10^5$ (s^{-1})	K_D (M)	Experimental method	References
7.0	0.28	4.0×10^{-14}	Radiolabled exchange reaction	Green (1990)
n.e.	n.e.	1.0×10^{-12}	Paramagnetic beads	Fujita and Silver (1993)
n.e.	n.e.	$\approx 10^{-10}$	Elisa	Chilkoti *et al.* (1995)
n.e.	n.e.	4×10^{-7}	Reflectometric interference spectroscopy	Piehler *et al.* (1996)
50	*	5.5×10^{-13}	SPR	Qureshi *et al.* (2001)
n.e.	n.e.	1.0×10^{-6}	Light scattering	Raschke *et al.* (2003)
n.e.	n.e.	1.0×10^{-11}	SPR	Haes and Van Duyne (2004)
460 ± 30	27 ± 5	$(5.8 \pm 0.7) \times 10^{-10}$	5 MHz QCM with impedance analysis	This work

n.e., constants not estimated.
*Off-rate not calculated and K_D obtained using k_{-1} published by Green in 1990.

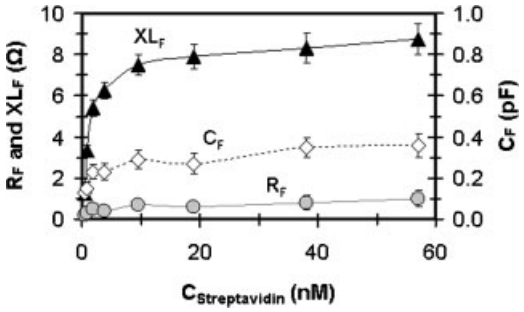

Figure 4. Impedance measurements for each streptavidin concentration. The inductance XL_F (Ω), resistance R_F (Ω) and parallel capacitance C_F (pF) contribution of streptavidin film to the BVD equivalent circuit, for each tested concentration ($\mu g\,ml^{-1}$).

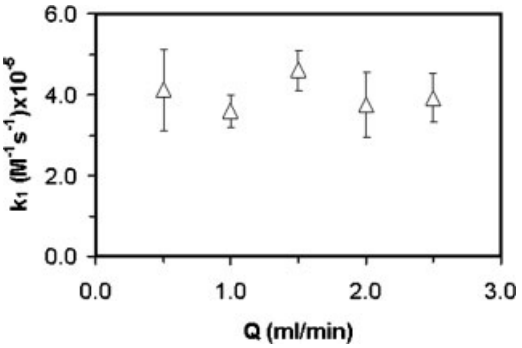

Figure 6. Dependence of the calculated streptavidin–biotin association kinetic constant k_1 to increasing flow rates of carrier buffer used during piezoelectric biosensing experiments. Each presented data are the average result of three independent experiments.

($k_{-1} = (0.3 \pm 5) \times 10^{-5}\,s^{-1}$) kinetic constants are estimated from the slope and the intercept of the linear relationship between the reciprocal of the binding relaxation time (τ^{-1}) and streptavidin solution concentration (Figure 5). While a good linear correlation was obtained for the variation of the reciprocal of the binding relaxation time (τ^{-1}) with the streptavidin solution concentration, which suggest the applicability of the 1:1 model, the association rate constant calculated is one order of magnitude lower as the one previously published estimated from surface plasmon resonance (SPR) data (Qureshi *et al*., 2001). The difference between these values can easily be explained by the fact that we verified the existence of a negative cooperativity in our biosensing system, leading to a situation where as the sensor surface becomes more and more saturated with target molecules, available adjacent binding sites may become less exposed leading to an apparent slower recognition process. To verify if the calculated kinetic parameters were also influenced by other mechanisms besides negative cooperativity, further investigation was carried out to determine the extent of the influence of mass transfer in the binding mechanism of streptavidin molecules to the biotin film. In order to do it, streptavidin binding experiments were performed with increasing flow rates, for it is known that in fluidic systems this can minimize the effects of mass transport phenomena (Kortt *et al*., 1997; Myszka *et al*., 1997; Barak-Shinar *et al*., 2000; Khaled and Vafai, 2004). Figure 6 shows that in fact the association kinetic constant does not change significantly with the increase in the carrier flow rate thus showing that for our biosensing system, diffusional effects do not exert a relevant influence on the calculated constants. Regarding the dissociation rate constant it was found to be lower then the associated experimental error removing any significance to the calculated constant. We ran thus in similar problems as for SPR determination (Qureshi *et al*., 2001) which are related to the limiting values that can be obtained for high affinity binding reactions where the desorption rate is very slow. The dissociation rate constant, however, can be calculated from the product of the dissociation equilibrium constant determined above ($K_D = (5.8 \pm 0.7) \times 10^{-10}$ M) to the association rate constant, yielding $k_{-1} = (2.7 \pm 0.5) \times 10^{-4}\,s^{-1}$. To our knowledge, this is the first dissociation rate constant calculated for the affinity binding of unlabelled streptavidin to immobilized biotin directly from measured data. Table 2 compares previously published data for streptavidin/biotin binding. The high affinity is indicated by the dissociation equilibrium constant, in the nano- to pico-molar range for most cases. Table 2 evidences the high dispersion of equilibrium constant values which are dependent on the experimental conditions and methodologies. Even though diffusional and cooperativity effects may contribute to this dispersion, it is mostly due to the very slow dissociation process, which, as also experienced by us, renders difficult the determination of dissociation rate constants from binding data. Nevertheless, the first published estimation of streptavidin/biotin binding constants were based on an extrapolation from experimental association rate constants of avidin binding to biotin, with a labelling strategy (Green, 1990), it still is most commonly used and referenced. Data reporting the experimental determination of streptavidin/biotin binding constants are scarce or make use of such extrapolated constants (Qureshi *et al*., 2001). In contrast, the approach reported in this paper enables the direct estimation of streptavidin/biotin binding constants using an acoustic based biosensing surface approach, without the need to label target molecules.

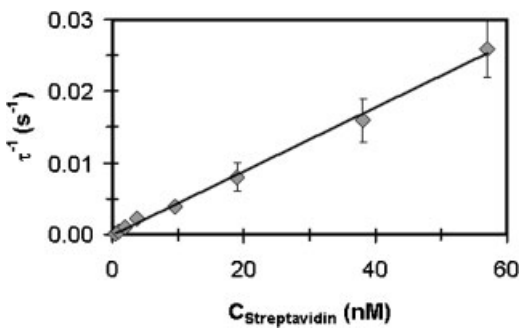

Figure 5. Linear dependence of the 1:1 molecular model calculated constant τ (relaxation time of binding), to the streptavidin concentrations used (0.5–57 nM). Linear regression of experimental data yielded the correlation: $\tau = (4.6 \pm 0.3) \times 10^5\,M^{-1}\,s^{-1} \times C + (0.3 \pm 5) \times 10^{-5}\,s^{-1}$; $r = 0.9882$; ANOVA analysis accepts linear interpolation for F statistic $p < 0.0001 < \alpha = 0.05$. Each presented data are the average result of three independent experiments.

CONCLUSIONS

In this work, piezoelectric sensors were used to study the process of 11-hydroxy-1-undecanothiol SAM formation and the recognition of streptavidin in aqueous medium.

By measuring simultaneously the resonant frequency variation and electroacoustic impedance of the sensors, quantitative analysis was enabled. Interfering signals from viscoelastic forces and electroacoustic coupling effects were found to be absent or negligible for the systems studied. Hence for both cases it was possible to directly use the Sauerbrey relationship for the analytical quantification of the mass adsorbed at the sensor surface, essential in data analysis tools based on models that necessary require this information. The approach used enabled the estimation of both kinetic and equilibrium binding constants with possible insights into the molecular mechanisms involved. Furthermore, it was shown that alkanethiol self-assembling process involves positive molecular cooperativity while, on the other hand, streptavidin binding to biotin involves negative cooperativity.

In summary, we have demonstrated that a full electroacoustic impedance analysis can significantly improve quantitative biosensing analysis with piezoelectric crystals in liquid environments. The modified equivalent circuit approach proposed can be further extended to the study of biomolecules with particular properties and even to potentially identify other surface molecular phenomena that can affect the response of piezoelectric sensors. This procedure can then easily be used in the study of affinity interactions, to identify interaction mechanisms, and/or to estimate equilibrium constants with a higher level of accuracy and confidence. This methodology thus potentially contributes to the future applicability of quartz crystal sensors in quantitative procedures like the evaluation of affinity pairs for separation applications, for the detection and quantification of molecules present in solution has a stand-alone analytical instrumentation and has a molecular screening technique in processes.

Acknowledgements

This work was supported by the Portuguese Science Foundation, an organism of the Portuguese Ministry of Science and Higher Education. Contracts number POCI/BIO/61912/2004 and POCI/QUI/63166/2004 are acknowledged. PhD grants number SFHR/BD/12772/2003 and SFHR/BD/17286/2004 to J. M. Encarnação and R. Baltazar are also acknowledged.

REFERENCES

Auge J, Hauptmann P, Hartmann J, Rösler S, Lucklum R. 1995. New design for QCM sensors in liquids. *Sens. Actuators B* **24**: 43–48.

Barak-Shinar D, Rosenfeld M, Zisman E, Abboud S. 2000. Computational fluid dynamic model of antigen–antibody surface adsorption on a piezoelectric immunosensor. *Ann. Biomed. Eng.* **28**: 565–571.

Bouché-Pillon D, Gabrielli C, Perrot H. 1995. Validation of the quartz-crystal microbalance response in liquid for sensor applications. *Sens. Actuators B* **25**: 257–259.

Chazenbalk G, Kakinuma A, Jaume J, McLachlan S, Rapoport B. 1996. Evidence for negative cooperativity among human thyrotropin receptors overexpressed in mammalian cells. *Endocrinology* **137**: 4586–4591.

Chilkoti A, Tan PH, Stayton PS. 1995. Site-directed mutagenesis studies of the high-affinity streptavidin-biotin complex: contributions of tryptophan residues 79, 108, and 120. *Proc. Natl. Acad. Sci. USA* **92**: 1754–1758.

Cooper MA, Singleton VT. 2007. A survey of the 2001 to 2005 quartz crystal microbalance biosensor literature: applications of acoustic physics to the analysis of biomolecular interactions. *J. Mol. Recognit.* **20**: 154–184.

Encarnação JM, Rosa L, Rodrigues R, Pedro L, Aires-da-Silva F, Gonçalves J, Ferreira GNM. 2007a. Piezoelectric biosensors for biorecognition analysis: Application to the kinetic study of HIV-1 Vif protein binding to recombinant antibodies. *J. Biotechnol.* **132**: 142–148.

Encarnação JM, Stallinga P, Ferreira GMN. 2007b. Influence of electrolytes in the QCM response: Discrimination and quantification of the interference to correct microgravimetric data. *Biosens. Bioelectron.* **22**: 1351–1358.

Etchenique R, Brudny VL. 2000. Characterization of porous thin films using quartz crystal shear resonators. *Langmuir* **16**: 5064–5071.

Etchenique R, Buhse T. 2000. Anomalous behaviour of the quartz crystal microbalance in the presence of electrolytes. *Analyst* **125**: 785–787.

Etchenique R, Weisz AD. 1999. Simultaneous determination of the mechanical moduli and mass of thin layers using nonadditive quartz crystal acoustic impedance analysis. *J. Appl. Phys.* **86**(4): 1994–2000.

Ewalt KL, Haigis RW, Rooney R, Ackley D, Krihak M. 2001. Detection of biological toxins on an active electronic microchip. *Anal. Biochem.* **289**: 162–172.

Ferreira GNM, Encarnação JM, Rosa L, Rodrigues R, Breyner R, Barrento S, Pedro L, Aires-da-Silva F, Gonçalves J. 2007. Recombinant single-chain variable fragment and single domain antibody piezoimmunosensors for detection of HIV1 virion infectivity factor. *Biosens. Bioelectron.* **23**: 384–392.

Fujita K, Silver J. 1993. Surprising Lability of Biotin-Streptavidin Bond During Transcription of Biotinylated DNA Bound to Paramagnetic Streptavidin Beads. *BioTechniques* **14**(4): 608–617.

Ghafouri S, Thompson M. 2001. Electrode modification and the response of the acoustic shear wave device operating in liquids. *Analyst* **126**: 2159–2167.

Green N. 1990. Avidin and streptavidin. *Meth. Enzymol.* **184**: 51–67.

Haes A, Van Duyne R. 2004. Preliminary studies and potential applications of localized surface plasmon resonance spectroscopy in medical diagnostics. *Expert Rev. Mol. Diagn.* **4**(4): 527–537.

Karpovich DS, Blanchard GJ. 1994. Direct measurement of adsorption kinetics of self-assembled monolayer films on a microcrystalline gold surface. *Langmuir* **10**: 3315–3322.

Khaled A, Vafai K. 2004. Optimization modeling of analyte adhesion over an inclined microcantilever-based biosensor. *J. Micromech. Microeng.* **14**: 1220–1229.

Kim DH, Noh J, Hara M, Lee H. 2001. An adsorption process study on the self-assembled monolayer formation of octadecanethiol chemisorbed on gold surface. *Bull. Korean Chem. Soc.* **3**(22): 276–280.

Kortt A, Gruen L, Oddie G. 1997. Influence of mass transfer and surface ligand heterogeneity on quantitative biacoretm binding data. Analysis of the interaction of NC10 Fab with an anti-idiotype Fab9. *J. Mol. Recognit.* **10**: 148–158.

Köβlinger C, Uttenthaler E, Drost S, Aberl F, Wolf H, Brink G, Stanglmaier A, Sackmann E. 1995. Comparison of the QCM and the SPR method for surface studies and immunological applications. *Sens. Actuators B* **24–25**: 107–112.

Laricchia-Robbio L, Revoltella RP. 2004. Comparison between the surface plasmon resonance (SPR) and the quartz crystal microbalance (QCM) method in a structural analysis of human endothelin-1. *Biosens. Bioelectron.* **19**: 1753–1758.

Liao S, Shnidman Y, Ulman A. 2000. Adsorption kinetics of rigid 4-mercaptobiphenyls on gold. *J. Am. Chem. Soc.* **122**: 3688–3694.

Liu Y, Zhang W, Yu X, Zhang H, Zhao R, Shangguan D, Li Y, Shen B, Liu G. 2004. Quartz crystal biosensor for real-time kinetic analysis of interaction between human TNF-α and monoclonal antibodies. *Sens. Actuators B* **99**: 416–424.

Lucklum R, Hauptmann P. 2000. The quartz crystal microbalance: mass sensitivity, viscoelasticity and acoustic amplification. *Sens. Actuators B* **70**: 30–36.

Martin S, Granstaff V, Frye G. 1991. Characterization of a quartz crystal. microbalance with simultaneous mass and liquid loading. *Anal. Chem.* **63**: 2272–2281.

Mitomo H, Shigematsu H, Kobatake E, Furusawa H, Ohahata Y. 2007. IgG binding kinetics to oligo B protein A domains on lipid layers immobilized on a 27 MHz quartz-crystal microbalance. *J. Mol. Recognit.* **20**: 83–89.

Modin C, Stranne A-L, Foss M, Duch M, Justesen J, Chevallier J, Andersen LK, Hemmersam AG, Pedersen FS, Besenbacher F. 2006. QCM-D studies of attachment and differential spreading of pre-osteoblastic cells on Ta and Cr surfaces. *Biomaterials* **27**: 1346–1354.

Muzykantov VR, Atochina EN, Gavriljuk V, Danilov SM, Fisher AB. 1994. Immunotargeting of streptavidin to the pulmonary endothelium. *J. Nucl. Med.* **35**: 1358–1365.

Myszka D, Morton T, Doyle M, Chaiken I. 1997. Kinetic analysis of a protein antigen-antibody interaction limited by mass transport on an optical biosensor. *Biophys. Chem.* **64**: 127–137.

Nesbitt W, Doyle R, Taylor K, Staat R, Arnold R. 1982. Positive cooperativity in the binding of Streptococcus sanguis to hydroxyapatite. *Infect. Immun.* **35**(1): 157–165.

Piehler J, Brecht A, Gauglitz G. 1996. Affinity detection of low molecular weight analytes. *Anal. Chem.* **68**: 139–143.

Porter MD, Bright TB, Allara DL, Chidseyi CED. 1986. Spontaneously organized molecular assemblies 4. Structural characterization of n-alkyl thiol monolayers on gold by optical ellipsometry, infrared spectroscopy, and electrochemistry. *J. Am. Chem. Soc.* **109**: 3559–3568.

Qureshi M, Yeung J, Wu S, Wong S. 2001. Development and characterization of a series of soluble tetrameric and monomeric streptavidin muteins with differential biotin binding affinities. *J. Biol. Chem.* **276**(49): 46422–46428.

Raschke G, Kowarik S, Franzl T, Sönnichsen C, Klar TA, Feldmann J, Nichtl A, Kurzinger K. 2003. Biomolecular recognition based on single gold nanoparticle light scattering. *Nano Lett.* **3**(7): 935–938.

Rosebrough SF, Hashmi M. 1996. Galactose-modified streptavidin-GC4 antifibrin monoclonal antibody conjugates: application for two-step thrombus/embolus imaging. *J. Pharmacol. Exp. Ther.* **276**: 770–775.

Sauerbrey G. 1959. The use of quartz oscillators for weighing thin layers and for microweighing. *Z. Phys.* **155**: 206–222.

Schechter B, Chen L, Arnon R, Wilchek M. 1999. Organ selective delivery using a tissue-directed streptavidin–biotin system: targeting 5-fluorouridine via TNP-streptavidin. *J. Drug Target.* **6**: 337–348.

Strong L, Whitesides GM. 1987. Structures of self-assembled monolayer films of organosulfur compounds adsorbed on gold single crystals: electron diffraction studies. *Langmuir* **4**: 546–558.

Su X-L, Li Y. 2005. A QCM immunosensor for Salmonella detection with simultaneous measurements of resonant frequency and motional resistance. *Biosens. Bioelectron.* **21**(6): 840–848.

Urizar E, Montanelli L, Loy T, Bonomi M, Swillens S, Gales C, Bouvier M, Smits G, Vassart G, Costagliola S. 2005. Glycoprotein hormone receptors: link between receptor homodimerization and negative cooperativity. *EMBO J.* **24**: 1954–1964.

Wu T-Z, Su C-C, Chen L-K, Yang H-H, Tai D-F, Peng K-C. 2005. Piezoelectric immunochip for the detection of dengue fever in viremia phase. *Biosens. Bioelectron.* **21**(5): 689–695.

Yang M, Yau HCM, Chan HL. 1998. Adsorption kinetics and ligand-binding properties of thiol-modified double-stranded DNA on a gold surface. *Langmuir* **14**: 6121–6129.

Yao Z, Zhang M, Kobayashi H, Sakahara H, Nakada H, Yamashina I, Konishi J. 1995. Improved targeting of radiolabeled streptavidin in tumors pretargeted with biotinylated monoclonal antibodies through an avidin chase. *J. Nucl. Med.* **36**: 837–841.

Zhou A, Zhang J, Xie Q, Yao S. 2000. Impedance analysis for the investigation of the behaviors of piezoelectric quartz crystal in the liquid at harmonic resonance. *Sens. Actuators B* **67**(1–2): 68–75.

